

Wide-Narrow Switchable Bands Microstrip Antenna for Cognitive Radios

Ros Marie C. Cleetus* and Gnanadhas Josemin Bala

Abstract—We introduce a six-switch integrated ultra wideband (UWB) — frequency reconfigurable system for cognitive radio applications. With respect to the requirements of the cognitive radio, this proposed design incorporates a UWB section for sensing the frequency spectrum, and the same design is frequency reconfigured using switches to get narrow bands for communicating within the spectrum. The proposed design has a compact size of $40\text{ mm} \times 40\text{ mm} \times 1.6\text{ mm}$ and is printed on an FR4 substrate with relative permittivity 4.4. The first configuration of switches allows the antenna to have UWB characteristics from 3.10 to 12 GHz and beyond as per simulations and 3.13 to 12 GHz and beyond as per measurements. Configurations II to V cover the ultrawide band from 3.54 to 12 GHz through five narrow bands. Measured results match well with the simulated ones. The comparative analysis of the antenna in terms of frequency reconfigurability is also included in this work which proves that the proposed design is an effective candidate for Cognitive Radio applications.

1. INTRODUCTION

In 2002, the Federal Communications Commission (FCC) decided the regulations for Ultra-Wideband (UWB) technology and assigned the unlicensed spectrum from 3.1 to 10.6 GHz for it. The significance of UWB antennas is increasing with the time, as the required data rates are high, the power requirements and the cost as low in the modern communication systems and increased security. The existence of a single UWB antenna is found to replace the need of a number of narrow band antennas [1, 2].

Reconfigurable antennas have gained a lot of focus in recent years. These antennas are able to modify themselves with respect to the characteristics, such as operating frequency, radiation pattern, polarization, and combinations of the above. A single reconfigurable antenna is capable of accommodating the features of a number of antennas. Notches in the reflection coefficient of the antenna make the antenna reconfigured in terms of frequency. Antennas once fabricated cannot be modified normally in operating bands. However, once these antennas are frequency reconfigured, they can be used to implement new services and bands. Also, such antennas have less effect of interference than wide-band antennas as they do not have the influence of bands not in use. It avoids the need of filters in such antennas, and the design part of the system becomes simplified [3]. The reconfigurability of the antennas is ensured by inserting switches like RF-MEMS, PIN diodes, varactors, photoconductive switches, etc. Physical alterations to the radiators as well as materialistic changes provide reconfigurability to the antenna. RF MEMS Switches are found to be dependable over microwave and millimeter-wave range applications with rapidness in switching, higher linearity and isolation, excellent adaptability, lower distortion rates, etc. [4–7]. PIN diodes and varactors are scalable and are able to respond within a few nanoseconds. Refined tuning is guaranteed by varactors, too. But the nonlinearity of the above switches is counted as a drawback [8, 9]. While electronic and mechanical switches are associated with losses due to bias lines and heaviness respectively, the photoconductive switches stand out in terms of

Received 28 October 2019, Accepted 23 December 2019, Scheduled 9 January 2020

* Corresponding author: Ros Marie C. Cleetus (rosmarie@sahrdaya.ac.in).

The authors are with the Karunya Institute of Technology & Sciences, Coimbatore, India.

no need of bias lines, higher switching speeds, improved isolation, easy fabrication, etc. [10, 11]. Physical alterations to achieve reconfigurability do not require bias lines, but become less competitive in terms of size, expenses, slower responses, etc. [12].

Usually, two antennas together will be used for spectrum sensing and signal transmission or reception. This makes the antenna size larger and complexity increased. Additional electromechanical devices may be needed so as to rectify many issues associated with the two antennas [13]. The proposed work can accommodate both the sensing and transmission/reception parts within the same design. Here, a rectangular patch frequency reconfigurable antenna is presented that can exhibit UWB characteristics as well as narrow band characteristics with the same design using various switching configurations. Switching between bands is achieved using frequency reconfiguration with six switches inserted into the extended transmission lines from the main feed line. The antenna design, results, comparison of the results of the proposed design with existing antenna systems are explained in the following sections.

2. ANTENNA CONFIGURATION: WORK PRINCIPLE AND DESIGN RULES

Microstrip patch antennas are found to have disadvantages in terms of narrow bandwidth and disability to work in multiple bands of frequencies. Most of the literatures reveal that when bandwidth is improved and multi-frequency operation allowed in an antenna, the gain will be compromised, or vice versa. Getting all these parameters at an appreciable level is a tough task [14]. This work makes use of reconfigurability with switches which allows this antenna to work in multiple bands with better bandwidth. The basic principle behind the antenna in this work is that the surface current distribution is varied with each of the 64 switching configurations of switches SW_1 to SW_6 , which in turn affects the operating frequency and radiation characteristics of each states. The configurations with better radiations and bandwidth are taken into account.

The top and bottom views of the proposed antenna design are illustrated in Fig. 1. A rectangle-shaped patch is used in the design because of its simplicity and easiness to design and fabricate. For the feeding of the antenna, a $50\ \Omega$ microstrip line is used. The rectangular patch is designed for a center frequency of 5.8 GHz. The substrate used for antenna designing is FR4-epoxy with dielectric constant 4.4 and thickness 1.6 mm. Using the above parameters, the design of the antenna is done with the design rules explained by Balanis [15]. The metallization of the antenna is done with the copper of thickness

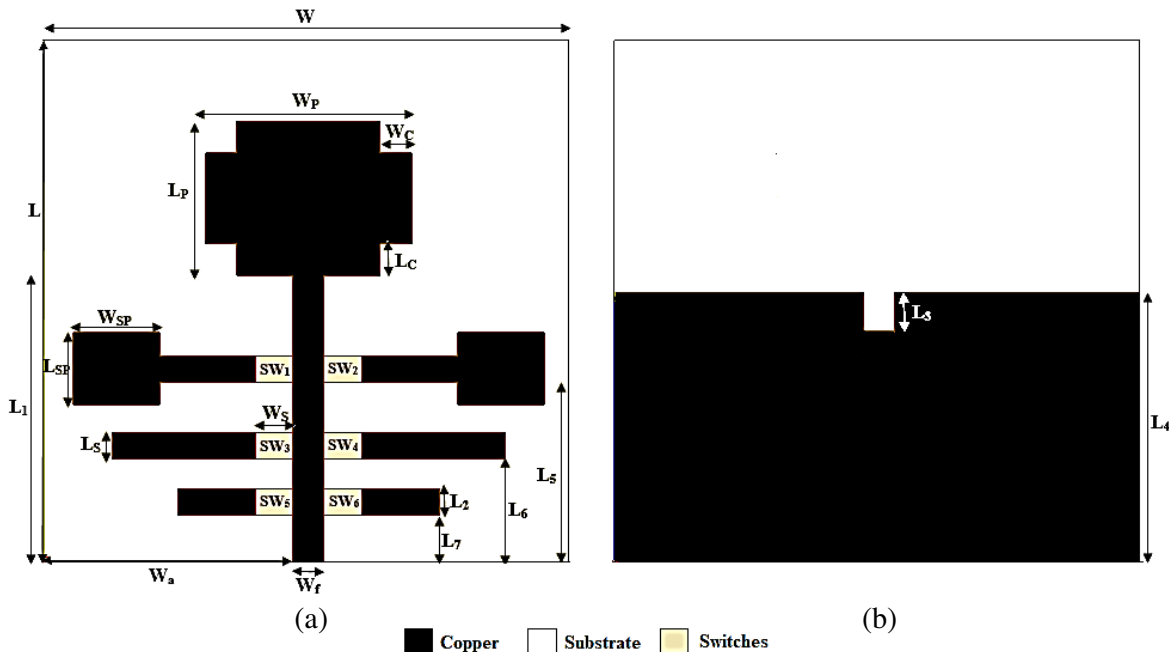


Figure 1. The antenna design. (a) Top view, (b) bottom view.

18 μm . The ground plane is made defective with a dimension of 40 mm \times 20.75 mm. The partial ground plane allows the antenna to work in the entire UWB range. Additionally, a slot of 2.36 mm \times 2.9 mm is cut from the ground plane, for impedance matching. Six extended transmission lines are inserted in the design that are allowed to be connected or disconnected to/from the main feed line by means of switches or conducting sheets. The simulations here are based on perfect electric conducting sheets. The sheets are inserted or removed for switching ON and OFF, respectively. The measurements are carried out in such a way that a copper tape of 18 μm thickness is cut into 6 pieces in the dimension of the switches of this design and used in place of Switches 1 to 6. These pieces are inserted or removed, into or from, the gap between the main feed line and extended transmission lines so as to obtain the ON state and OFF state of the switches, respectively. The switching can be carried out using MEMS switches. It could be observed from the simulations that with the use of six Radant MEMS SPST-RMSW100 switches instead of conducting sheet switches, the antenna exhibits similar radiating properties. These switches are modeled as $< 1 \Omega$ resistor for ON state and $> 1 \text{ G}\Omega$ resistor for OFF state in the HFSS Software. With 6 switches, the design is able to provide 64 configurations from all switches OFF to all switches ON. The surface current distributions are different for different configurations. Hence, the operating frequencies will also be different. The configuration with all the switches in OFF condition, i.e., with no extended transmission lines connected, is termed as Configuration I. The other configurations tend to provide narrow bands with varying operating frequencies within the UWB spectrum. The front and back views of the fabricated antenna are shown in Fig. 2.

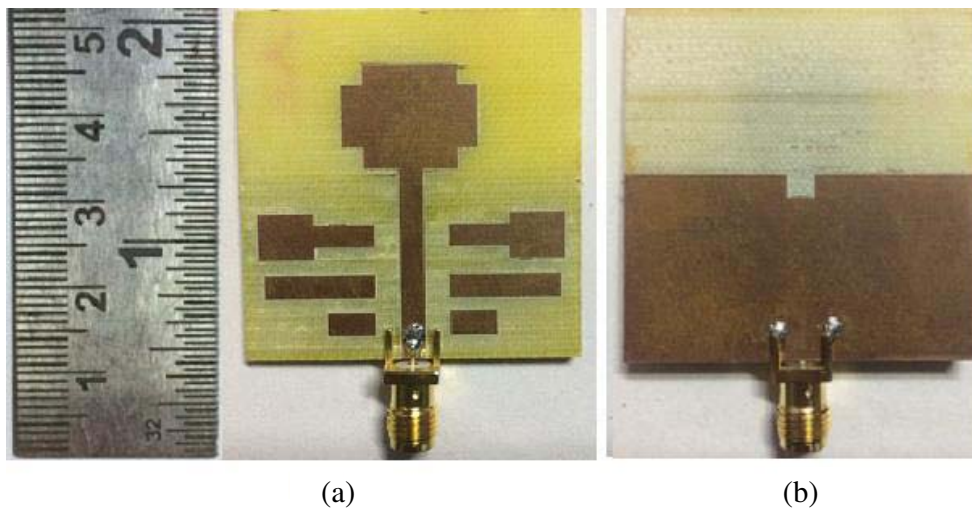


Figure 2. Fabricated antenna. (a) Front view, (b) back view.

3. PARAMETRIC STUDY

The dimensions of the antenna have been varied to obtain optimal responses, and the corresponding reflection characteristics of the antenna are studied here. A few of such variations are considered in this paper.

3.1. Variation of Slot Length L_3

Slot length L_3 is varied from 2.7 mm to 3 mm with a 0.1 mm difference. The results of the parametric study with all the switches in OFF condition are included in Fig. 3. All the cases give UWB responses. Even though the values of L_3 as 2.7 mm, 2.8 mm, and 3 mm are found to return UWB responses, they tend to exhibit poor S_{11} against frequency 8 to 9 GHz. Out of these, slot length 2.9 mm is found to return an optimal response. As the length of the slot introduced in the ground plane increases from 0 mm to L_3 mm (2.9 mm), on a continual basis, matching is found improved. The input impedance

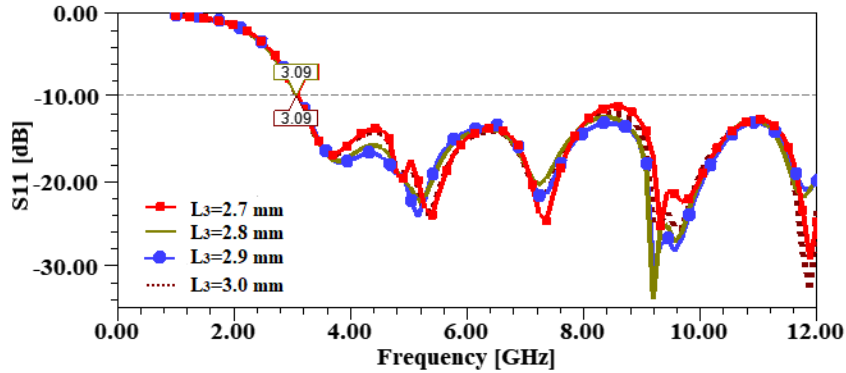


Figure 3. Simulated reflection characteristics of UWB with variation of slot length.

reaches near 50Ω and maximum power transfer to the antenna happens. It results in better reflection characteristics at L_3 as 2.9 mm. Further increase in L_3 does not contribute to matching. So, it could be stated that a slot cut on the ground plane, with the same width of the main feed line and length 2.9 mm, allows the antenna to work with better UWB characteristics than no slot cut on the ground plane as well as a slot cut with lengths less than or greater than 2.9 mm.

3.2. Variation of Length of Defected Ground Plane L_4

The ground plane lying below the entire substrate usually makes any antenna to cover narrow band(s) only, whereas a monopole antenna printed over a defective ground plane covers a wide band of frequencies. The length of the defective ground plane plays a significant role in determining the bandwidth of the antenna. In the parametric study, the length of the ground plane is varied through four values, 20.65 mm, 20.75 mm, 20.85 mm, and 20.95 mm. All switches OFF condition is depicted in Fig. 4. Even though it could not be included in this article, the parametric study has covered a wider range of L_4 , from 10 mm to 25 mm. The antenna is found to exhibit UWB characteristics at around the length equal to 20 mm. As the length of the ground plane increases further, the antenna has the tendency to lose its UWB characteristics and exhibits multi-band characteristics. All the four values indicated in Fig. 4 return UWB characteristics, whereas an excellent response in the UWB range is obtained with the value of 20.75 mm.

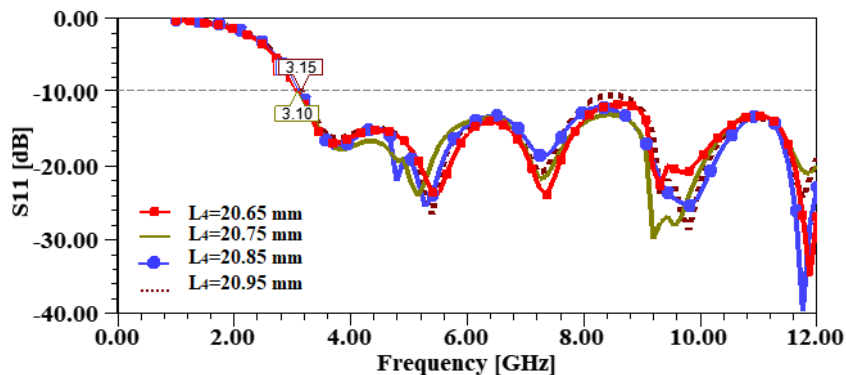


Figure 4. Simulated reflection characteristics of UWB with variation of defected ground plane length.

3.3. Variation of Slot Dimensions L_C & W_C

The dimensions of the slots cut from the four corners of the main rectangular patch are varied from 2.2 mm to 2.5 mm with 0.1 mm separation in between values. The responses are shown in Fig. 5. The shape of the patch is varied from the usual rectangular shape that affects the entire electrical length

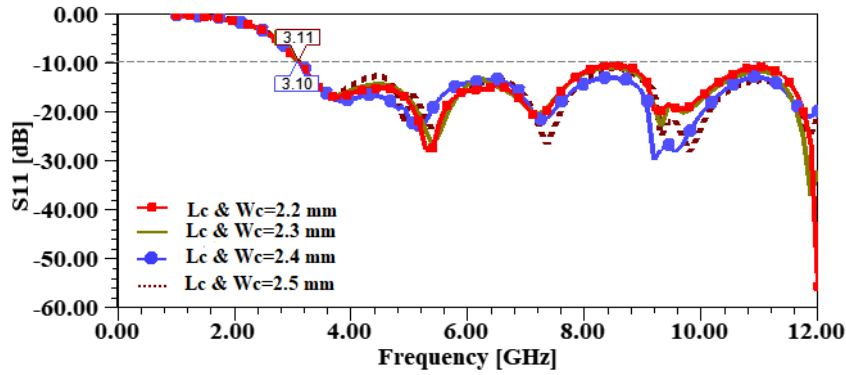


Figure 5. Simulated reflection characteristics of UWB with variation of slot dimensions.

and hence the surface current. Rectangular slots introduced in the patch edge increase the electrical length of the patch, and it improves the bandwidth of the antenna. The patch with no slots cut at the edges does not seem to provide exact entire UWB coverage. Even though all the mentioned dimensions result in UWB responses, the values 2.2 mm, 2.3 mm, and 2.5 mm make the antenna have lower return loss that is very close to -10 dB in the range 8 to 9 GHz. Optimal response of UWB for all the switches OFF in condition is obtained with the value at 2.4 mm.

From the above parametric studies, it can be concluded that in all the above cases, variations in dimensions of the slots and conducting sheets effectively change the electrical length, and the increase in the electrical length results in a corresponding increase in the surface current of the structure which in turn improves the bandwidth of the structure. With reference to the above and a number of parametric studies conducted, the dimensions of the antenna structure are finalized and enlisted in Table 1.

Table 1. Dimensions of the antenna (All dimensions are in mm).

L	L_1	L_2, L_S	L_3	L_4	L_5	L_6	L_7	L_P
40.00	22.07	2.00	2.90	20.75	14.00	8.16	3.86	11.75
W	W_f	W_a	W_S	W_P	W_{SP}	L_{SP}	W_C	L_C
40.00	2.36	19.00	2.90	15.74	6.61	5.53	2.40	2.40

4. RESULTS AND DISCUSSIONS

Out of the 64 combinations possible from the six switches, the switching configurations of the six switches to attain ultra-wideband and narrow band characteristics are listed in Table 2. Simulations based on switches as perfect electric conducting sheets (pec sheets) as well as Radant MEMS SPST-RMSW100 models and measurements with the perfect electric conductor, copper sheets are carried out in this work. A superimposition of the simulated and measured reflection characteristics of the antenna for Configurations I to V are depicted from Fig. 6 to Fig. 10. The frequency band, bandwidth, and the corresponding return loss obtained for the Configurations mentioned in Table 2 are listed in Table 3.

The rectangular patch, with slots cut at the four corners of the patch, is found to exhibit UWB response according to Fig. 6, even in the presence of extended transmission lines lying on the same plane. The return loss maintains < -10 dB within the UWB range. The first configuration, with all switches in OFF condition, tends to cover the entire UWB (3.10 to 10.6 GHz) in both cases of simulations, whereas it starts coverage at 3.13 GHz when it comes to the measured results. When the switching status is changed from all OFF to at least one is ON, the antenna turns out to be a narrow band antenna exhibiting frequency reconfigurable nature. The reconfigurability illustrated from Fig. 7 to Fig. 10 provides coverage of UWB as narrow bands from 3.54 to 10.6 GHz as per simulation using perfect

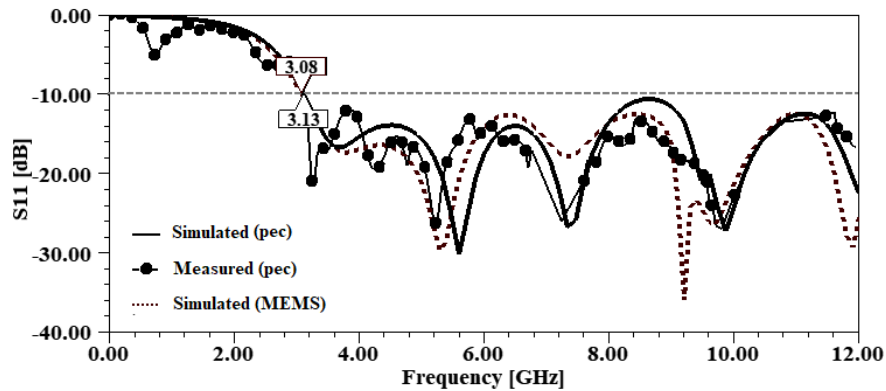


Figure 6. Reflection characteristics of Configuration I.

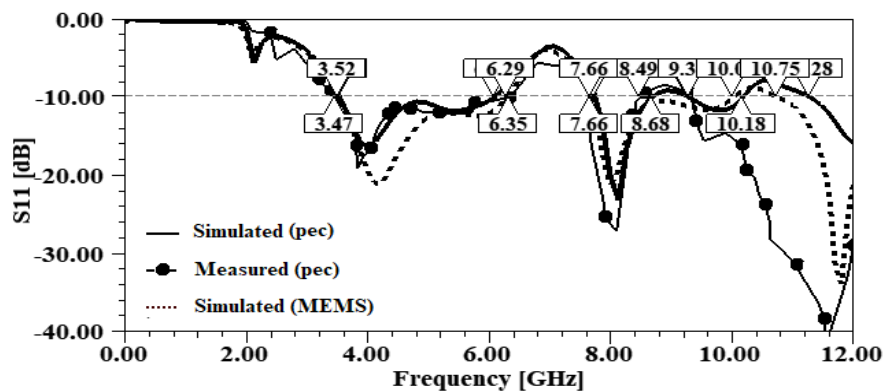


Figure 7. Reflection characteristics of Configuration II.

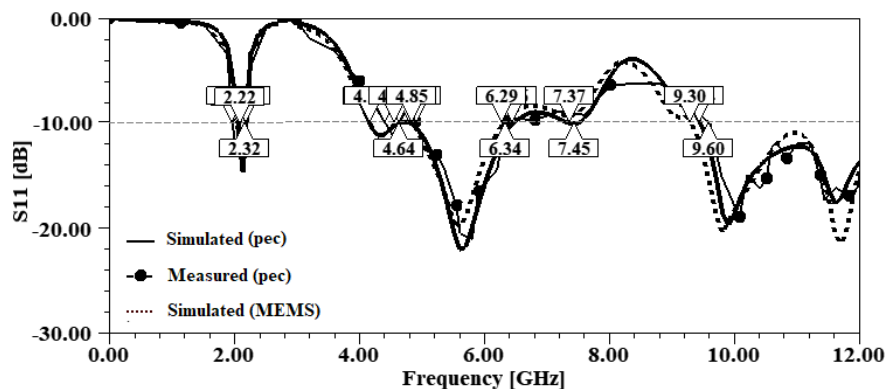


Figure 8. Reflection characteristics of Configuration III.

electric conducting sheet switches, 3.52 to 10.6 GHz according to simulations by Radant MEMS SPST-RMSW100 switches and 3.47 to 10.6 GHz with respect to the measurement using copper sheet switches in the order Configurations II, III-1, IV, V, and III-2, respectively. Meanwhile, Configuration III-1 does not contribute to the narrow band coverages in simulation using MEMS switches and measurements using copper sheets, as these are already taken up by the coverage of Configuration II in both of these cases. Configuration II seems to provide three narrow bands within the UWB range, and still the band providing coverage from 3.54 to 6.09 GHz only is considered. The other narrow bands from Configuration II are omitted, as those are better covered by Configuration V with good return loss

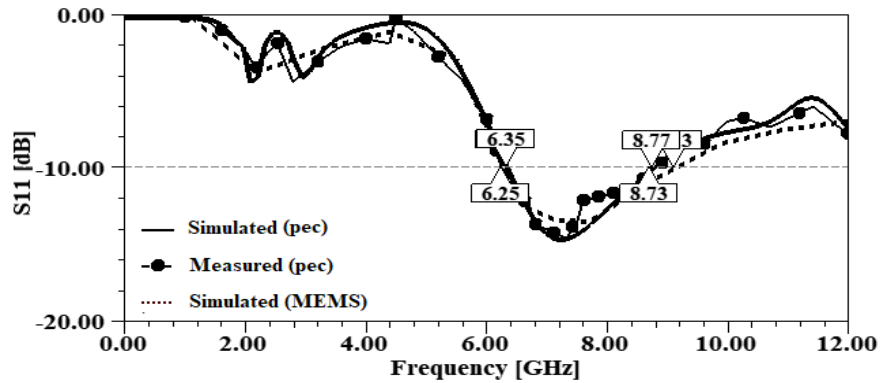


Figure 9. Reflection characteristics of Configuration IV.

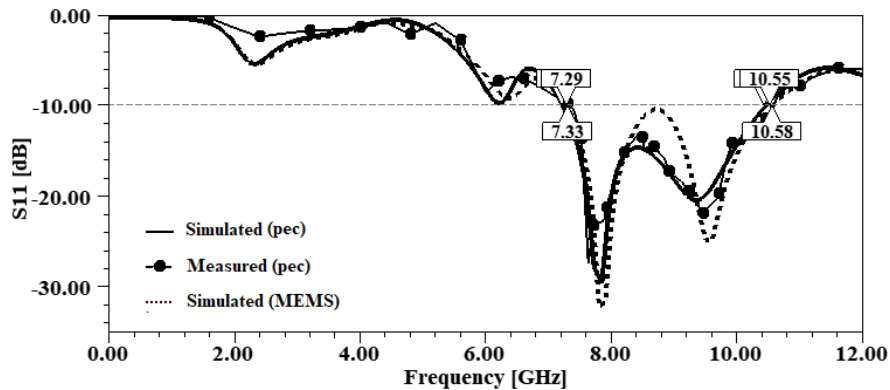


Figure 10. Reflection characteristics of Configuration V.

Table 2. Switching configurations.

Configuration	SW ₁	SW ₂	SW ₃	SW ₄	SW ₅	SW ₆
I	OFF	OFF	OFF	OFF	OFF	OFF
II	ON	OFF	OFF	OFF	OFF	OFF
III	OFF	OFF	OFF	ON	OFF	OFF
IV	OFF	ON	OFF	ON	ON	OFF
V	OFF	OFF	OFF	OFF	ON	OFF

characteristics and bandwidth. Configurations II, III-1, and III-2 maintain nearly -20 dB return loss for both the simulations and measurement. Configuration V, in all the cases, maintains a good level of impedance matching with nearly -30 dB return loss in all the three scenarios, whereas configuration IV performs comparatively weaker with almost -15 dB return loss in simulations and measurement. All the considered configurations for narrow band performance occupy good bandwidth from greater than 1 to greater than 3 GHz.

Simulations in both switching scenarios, i.e., with pec sheets and MEMS switches, are found in good agreement. The measurements using copper sheet switches get along with the above-mentioned simulations. Slight variations have occurred that are expected to happen with the minor faults in fabrication, measurement, and losses associated with the connector and material. In the case of MEMS switches, even though the modeling by HFSS does not consider the losses associated with the packaging of real switches, it is expected that the simulations and measurements will not differ much.

Table 3. Simulated and measured results.

Config.	Simulation (Using pec sheets)			Simulation (Using MEMS Switches)			Measurement (Using copper sheets)		
	Frequency (GHz)	Bandwidth (GHz)	Return Loss (dB)	Frequency (GHz)	Bandwidth (GHz)	Return Loss (dB)	Frequency (GHz)	Bandwidth (GHz)	Return Loss (dB)
I	3.10 to 12 GHz and beyond	8.9	< -10	3.08 to 12 GHz and beyond	8.92	< -10	3.13 to 12 GHz and beyond	8.87	< -10
II	3.54 to 6.09	2.55	-16.34	3.52 to 6.29	2.77	-20.63	3.47 to 6.35	2.88	-19.04
III-1	4.81 to 6.46	1.65	-22.1	4.85 to 6.29	1.44	-19.63	4.92 to 6.34	1.42	-20.96
III-2	9.44 to 12.00	2.56	-19.60	9.30 to 12	2.70	-21.07	9.60 to 12.00	2.40	-18.89
IV	6.35 to 8.77	2.42	-14.6	6.32 to 9.13	2.81	-13.39	6.25 to 8.73	2.48	-14.55
V	7.22 to 10.45	3.23	-29.5	7.29 to 10.55	3.26	-32.02	7.33 to 10.58	3.25	-27.21

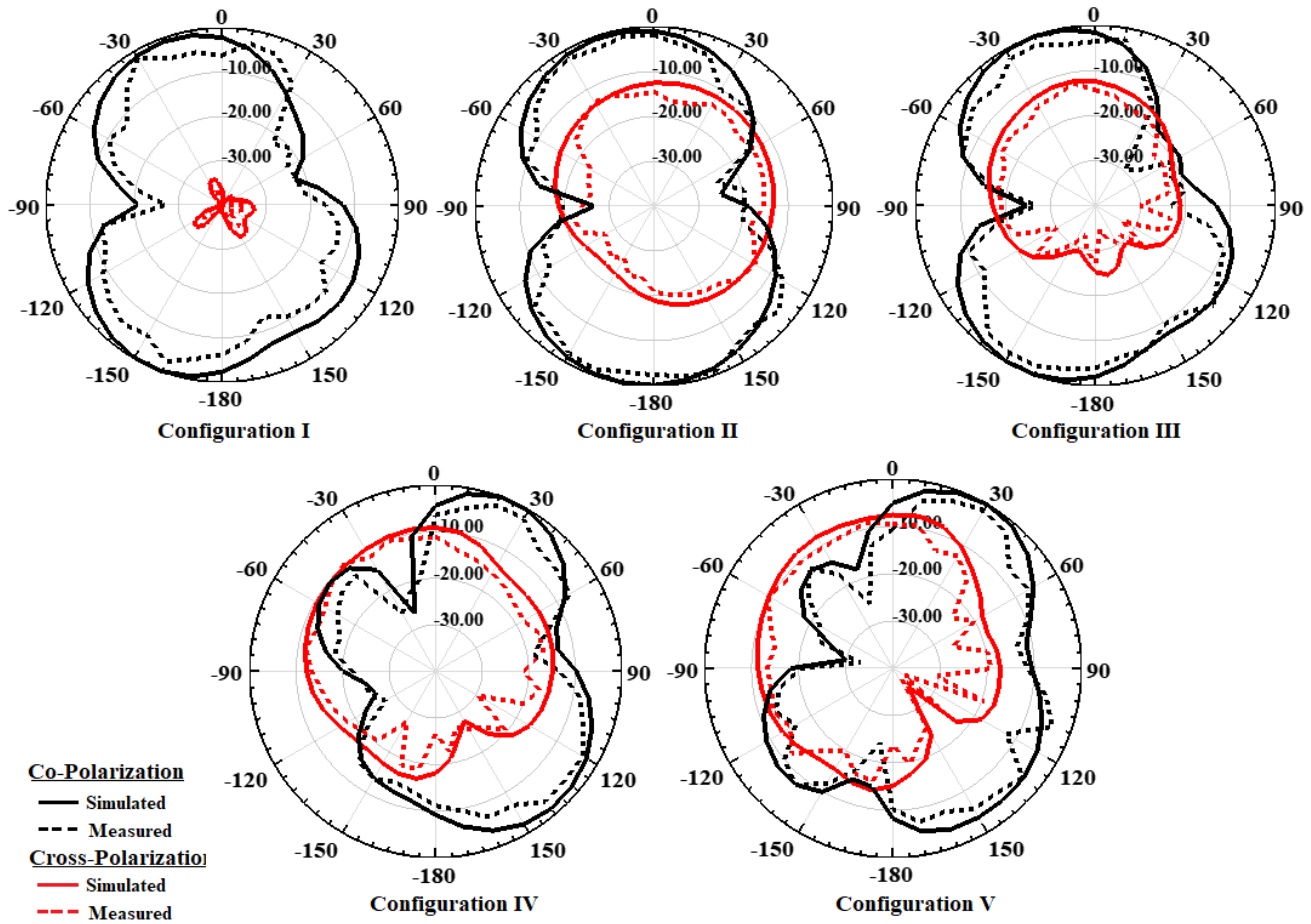


Figure 11. Simulated and measured normalized radiation pattern in the *E* plane for Configurations I to V.

For each configuration, simulated and measured normalized co-polarization and cross-polarization patterns in the *E* plane and *H* plane are shown in Fig. 11 and Fig. 12, respectively. The pattern is based on the frequency with the lowest reflection characteristics in each configuration. For Configurations I to V, they are 5.8 GHz, 4 GHz, 5.6 GHz, 7.2 GHz, and 7.8 GHz, respectively. The simulations and measurements are in good agreement.

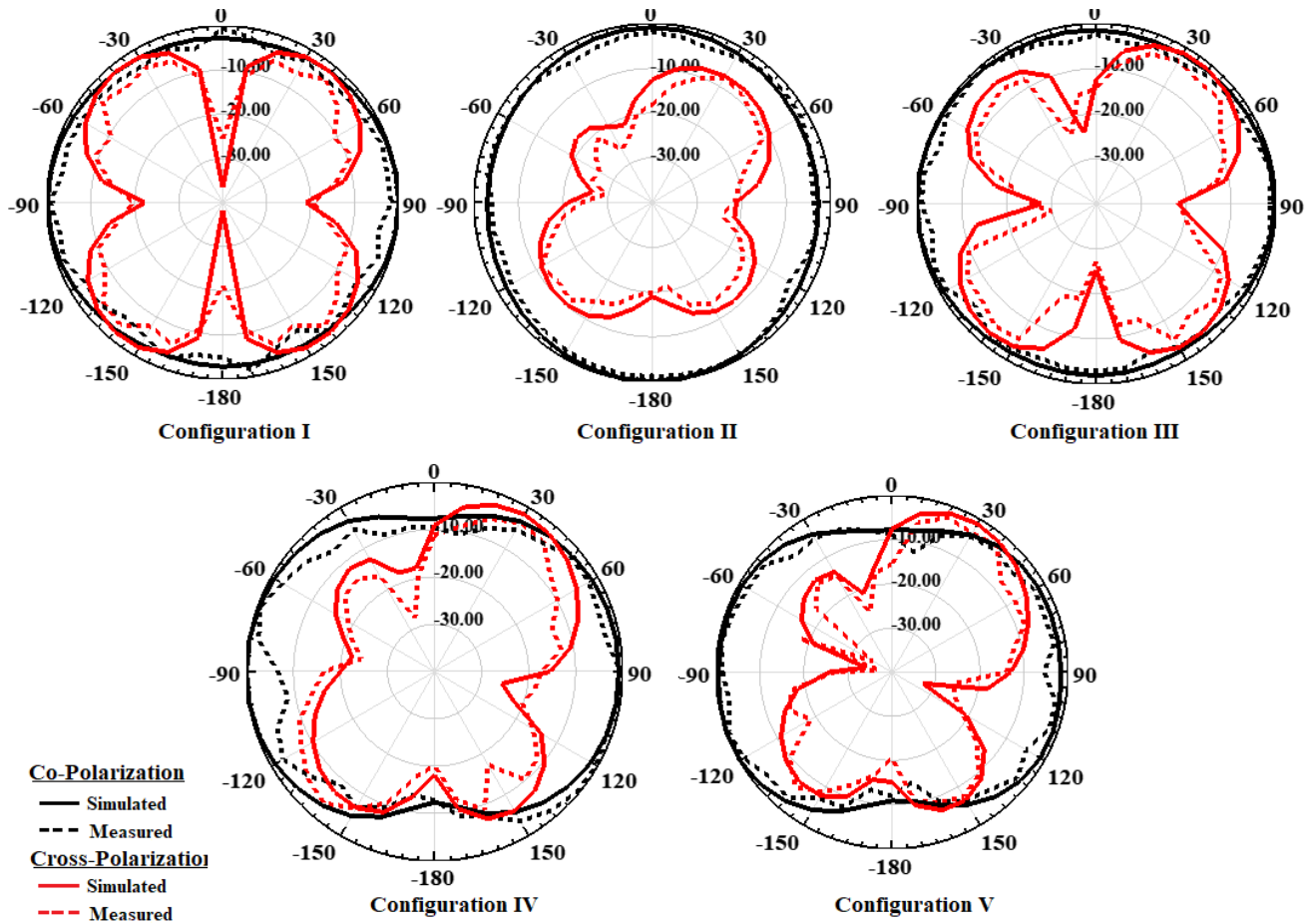


Figure 12. Simulated and measured normalized radiation pattern in the H plane for Configurations I to V.

Table 4. Comparison of the proposed system with existing systems.

References	Size (mm ³)	Ultra wideband (GHz)	Narrow bands (GHz)
[4]	30 × 30 × 1.6	3.2–12	3.3–4.1
[13]	40 × 40 × 1.6	3.1–10.6	6.55–6.64, 3.5–4.3, 8.34–8.87, 5.44–6.18, 7.43–7.63, 10.15–10.65
[16]	60 × 120 × 1.5	0.75–7.65	1.77–2.51
[17]	29 × 28	3.1–10.6	3.46–5.96, 3.28–6.26, 9.04–9.526
[18]	20 × 25.32 × 1.6	1.9–29.5	9.2–10.4
[19]	33 × 24 × 1.6	3.1–10.7	3.31–3.74, 5.03–5.94
[20]	37 × 63.6 × 0.254	2–12	5.7–5.9
[21]	30 × 30 × 1.6	3.1–10.6	6.36–6.63, 8.78–9.23, 7.33–7.7, 9.23–9.82
[22]	40 × 38.5 × 0.5	3–11	5.8–6.8, 6.7–7.3, 7.0–8.4, 7.9–9.2
[23]	40 × 36 × 0.662	3–11	Three bands in between 5 and 6 GHz
[24]	68 × 54 × 0.79	3–11	4.9–5.35, 4 GHz, 8 GHz, 10 GHz
[25]	58 × 65.5 × 1.6	3.3–11	3.4–4.85, 5.3–9.15
Proposed System	40 × 40 × 1.6	3.10 to 12 GHz and beyond	Entire Spectrum from 3.54–10.6 GHz (5 narrow bands)

At Configuration I, for the operating frequency 5.8 GHz, the co-polarization pattern in E plane resembles that of a dipole antenna, and that of H plane is omnidirectional. The presence of the defected ground plane provides such a shape of pattern to this design. A printed monopole placed over a partial ground surface ensures the omnidirectional nature of the pattern. The cross-polarization levels in both the cases are less than that of co-polarization levels. The other configurations with varied operating frequencies do not provide similar pattern shapes and offer varying shapes as they are not symmetrical in structure. Configurations II and III, both centered at frequencies lower than 5.8 GHz, at 4 GHz and 5.6 GHz respectively, indicate slight variation in the co-polarization levels from that of Configuration I. Configuration III tends to follow almost a similar shape as it operates very close to the designated frequency of the antenna. But as antenna operates in frequency bands other than 5.8 GHz, an increase happens in cross-polarization levels because the antenna operates at a distant frequency range from the one that it is actually designed. When the antenna operates at frequencies greater than 5.8 GHz, in Configurations IV and V (centered at 7.2 GHz and 7.8 GHz respectively), the pattern is modified to directional in nature. The major lobe exhibits deviations from the broadside direction. Also, the levels of radiations are comparatively less than that from Configurations I, II, and III. It can

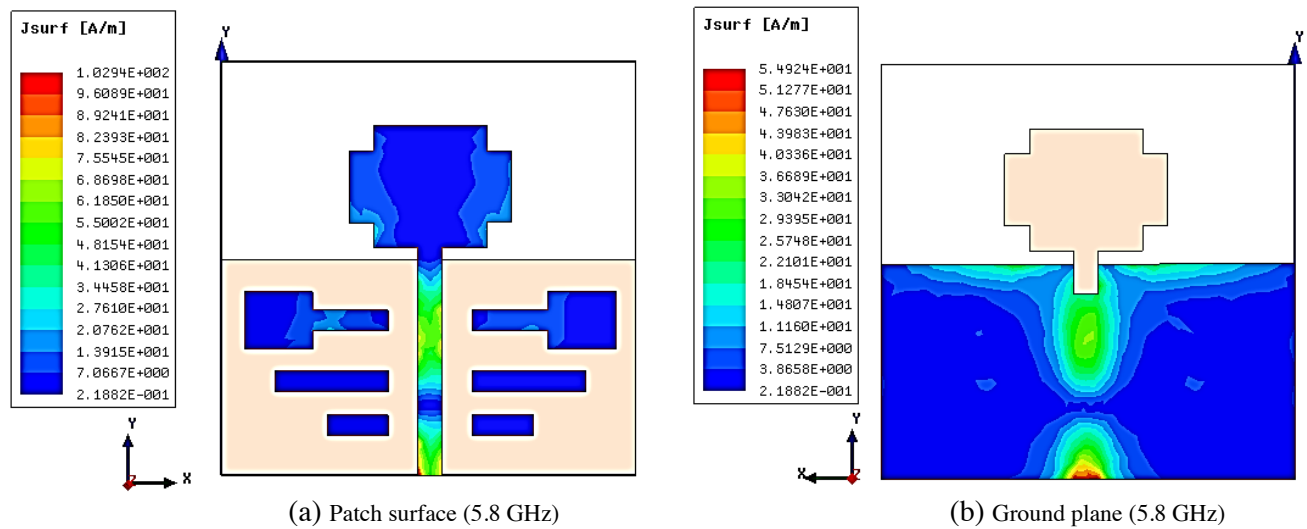


Figure 13. Surface current distribution of Configuration I.

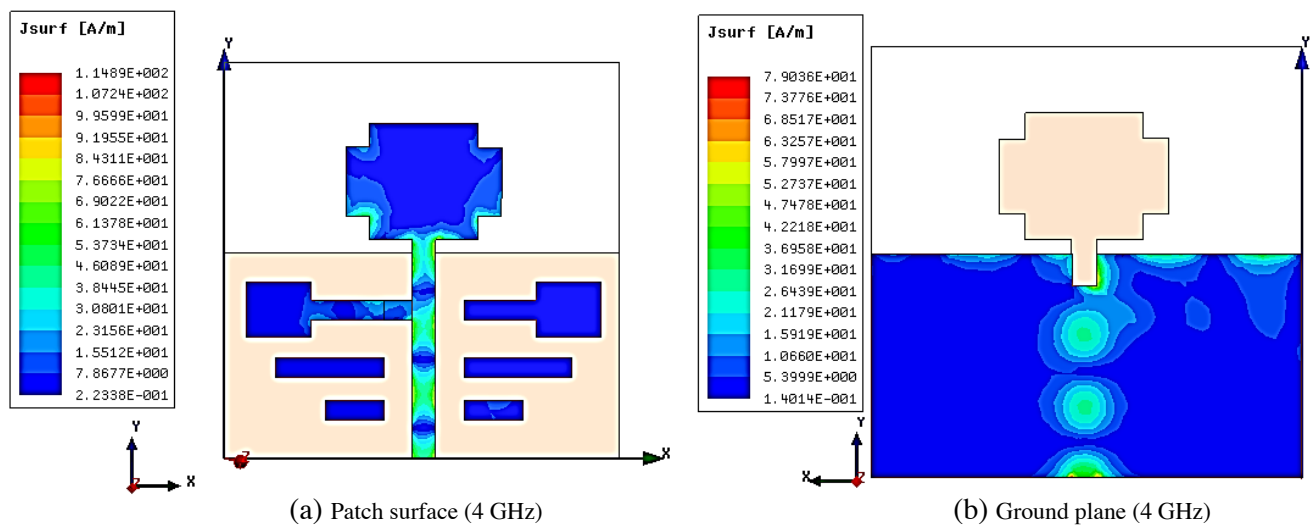


Figure 14. Surface current distribution of Configuration II.

be better concluded that as the frequency increases from the designed frequency, the antenna loses its omnidirectional nature, and the E plane patterns are found to have side lobes.

The antenna parameter peak gain, computed using HFSS, is found to be 1.14 dB at 5.8 GHz for Configuration I, 2.8 dB at 4 GHz for Configuration II, 1.24 dB at 5.6 GHz for Configuration III, 2.74 dB at 7.2 GHz for Configuration IV, and 2.24 dB at 7.8 GHz for Configuration V.

The comparison of the proposed system with existing systems is given in Table 4. Compared to other works in the same area, the proposed antenna exhibits the characteristics of a UWB antenna that can cover the entire UWB spectrum (3.10 to 10.6 GHz) and also of frequency reconfigurable antenna with 5 narrow bands from 3.54 to 10.6 GHz. None of the referred designs performs as better as the proposed work. It makes this antenna a suitable candidate for Cognitive Radio applications with spectrum sensing and communicating properties.

To interpret the behavior of the antenna, the surface distributions of current in both the patch surface and the defected ground plane for corresponding resonance frequencies of the selected five configurations, 5.8 GHz, 4 GHz, 5.6 GHz, 7.2 GHz, and 7.8 GHz respectively, are shown in Fig. 13, Fig. 14, Fig. 15, Fig. 16, and Fig. 17. The magnitudes of surface current at the patch surface and

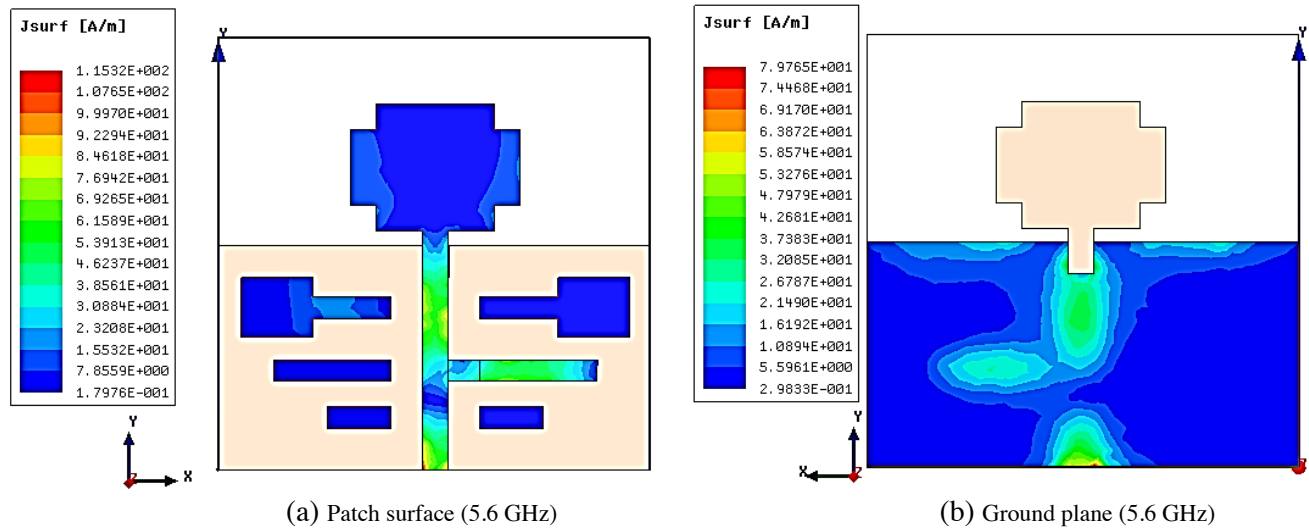


Figure 15. Surface current distribution of Configuration III.

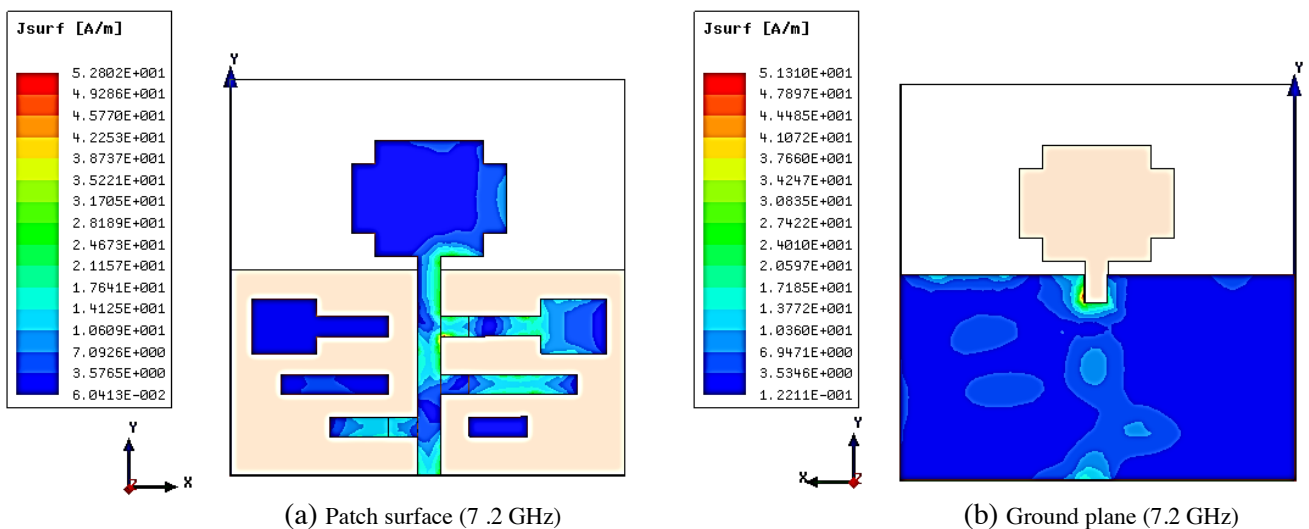


Figure 16. Surface current distribution of Configuration IV.

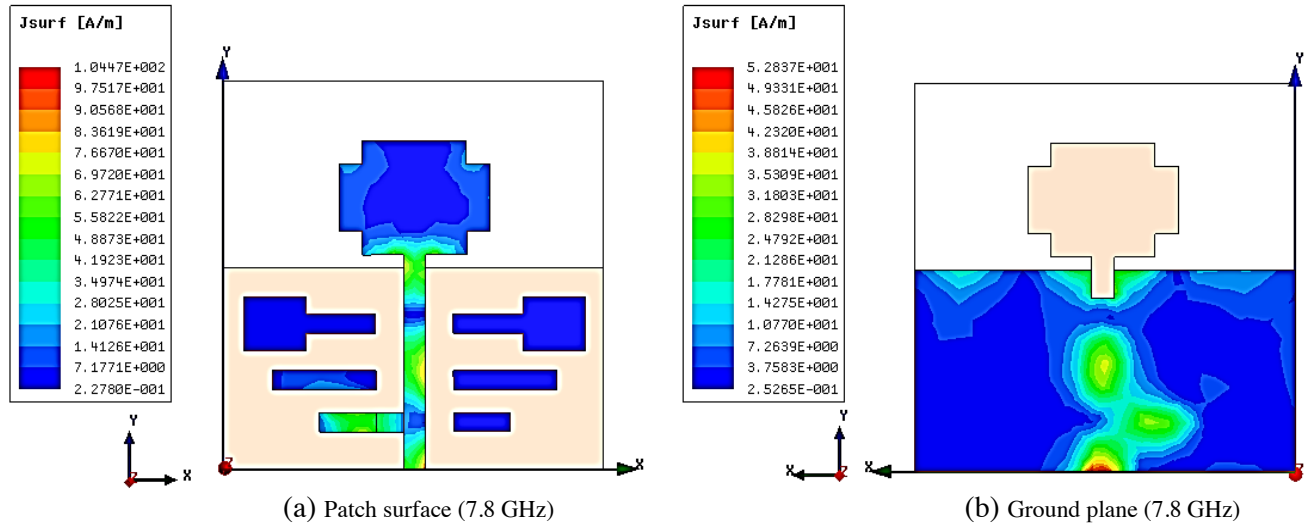


Figure 17. Surface current distribution of Configuration V.

ground plane are simulated by the field plotting option of the HFSS software. At times, switches are ON and OFF, and the current distribution can be seen varied. As no extended transmission lines are connected to the main feed line in Configuration I, the current distribution is confined to the main feed line, whereas in other configurations as various extended transmission lines are connected via switches to the main line, the surface current is also distributed to the extensions. It is explicit from Fig. 13 to Fig. 17 that most of the current distribution is centered at the lower edge of the antenna. It is the edges that mainly contribute to the radiations of the antenna. The slots cut at the corners of the patch does not affect the radiations of the antenna much, whereas the edge formed by cutting slot on the ground plane shows that the current distribution varies well with respect to it.

5. CONCLUSION AND FUTURE WORK

This paper reports a frequency reconfigurable antenna that can be reconfigured as an UWB antenna and narrow band antennas. The reconfigurability can be achieved using 6 switches inserted into the design which will, in turn, connect or disconnect the extended transmission lines to or from the main feed line. Configuration I with all switches OFF combination allows the antenna to operate in the UWB (3.1 to 10.6 GHz). Configurations II, IV, and V ensure single band operation whereas Configuration III gives a double band operation. These 4 configurations, i.e., Configuration II, III, IV, and V, collectively allow the antenna to operate from 3.54 to 10.6 GHz as five narrow bands. Measured results show good agreement with the simulated ones throughout. Configuration I makes the antenna suitable for spectrum sensing part of Cognitive Radio, and Configurations II to V allow the antenna to be used for communicating within the UWB spectrum. Hence the antenna becomes a good, self-sufficient candidate for Cognitive Radio applications. As a future expansion, the switching technique of this design can be replaced by the proposed MEMS switches and can validate the results. As of now, according to the available resources, not any designs with the electrical reconfiguration technique serve the requirement of the communicating section of the Cognitive Radio fully. So, it is suggested that as an extension to this design, a parametric analysis shall be conducted in the placement of feed lines and their dimensions to ensure entire UWB coverage through narrow bands for the communicating section of the Cognitive Radio.

REFERENCES

1. Liang, X. L., "Chapter 7: Ultra wideband current status and future trends," *Ultra Wideband Antenna and Design*, 127–152, 2012.

2. Fontana, R., "Recent system applications of short-pulse ultra-wideband (UWB) technology," *IEEE Trans. Microw. Theory Techn.*, Vol. 52, No. 9, 2087–2104, 2004.
3. Li, T., H. Zhai, X. Wang, L. Li, and C. Liang, "Frequency-reconfigurable bow-tie antenna for Bluetooth, WiMAX, and WLAN applications," *IEEE Antennas Wireless Propag. Lett.*, Vol. 14, 171–174, 2015.
4. Ibrahim, A. A., A. Batmanov, and E. P. Burte, "Design of reconfigurable antenna using RF MEMS switch for cognitive radio applications," *2017 Progress In Electromagnetics Research Symposium — Spring (PIERS)*, 369–376, St Petersburg, Russia, May 22–25, 2017.
5. Abirami, M. and G. Rajasekar, "MEMS reconfigurable slotted microstrip patch antenna for cognitive radio application," *2016 Online International Conference on Green Engineering and Technologies (IC-GET)*, 2016.
6. George, R., C. R. Kumar, and S. Gangal, "Design of a frequency reconfigurable pixel patch antenna for cognitive radio applications," *2016 International Conference on Communication and Signal Processing (ICCSP)*, 1684–1688, 2016.
7. Wu, T., R. L. Li, S. Y. Eom, S. S. Myoung, K. Lim, J. Laskar, and M. M. Tentzeris, "Switchable quad-band antennas for cognitive radio base station applications," *IEEE Trans. Antennas Propag.*, Vol. 58, No. 5, 1468–1476, 2010.
8. Hussain, R. and M. S. Sharawi, "Planar meandered-F-shaped 4-element reconfigurable multiple-input-multiple-output antenna system with isolation enhancement for cognitive radio platforms," *IET Microwaves, Antennas Propagation*, Vol. 10, No. 1, 45–52, 2016.
9. Ge, L., M. Li, J. Wang, and H. Gu, "Unidirectional dual-band stacked patch antenna with independent frequency reconfiguration," *IEEE Antennas Wireless Propag. Lett.*, Vol. 16, 113116, 2017.
10. Andy, A., P. Alizadeh, K. Z. Rajab, T. Kreouzis, and R. Donnan, "An optically-switched frequency reconfigurable antenna for cognitive radio applications," *2016 10th European Conference on Antennas and Propagation (EuCAP)*, 2016.
11. Tawk, Y., J. Costantine, S. Hemmady, G. Balakrishnan, K. Avery, and C. G. Christodoulou, "Demonstration of a cognitive radio front end using an optically pumped reconfigurable antenna system (OPRAS)," *IEEE Trans. Antennas Propag.*, Vol. 60, No. 2, 1075–1083, 2012.
12. Tummas, P., P. Krachodnok, and R. Wongsan, "A frequency reconfigurable antenna design for UWB applications," *2014 11th International Conference on Electrical Engineering/Electronics, Computer, Telecommunications and Information Technology (ECTICON)*, 2014.
13. Rodrigues, E. J., H. W. Lins, and A. G. D'Assuncao, "Reconfigurable circular ring patch antenna for UWB and cognitive radio applications," *The 8th European Conference on Antennas and Propagation (EuCAP 2014)*, 2014.
14. Li, F. and T. Wang, "Design of reconfigurable UWB microstrip antenna with MEMS switches," *2016 IEEE International Conference on Microwave and Millimeter Wave Technology (ICMMT)*, 740–742, 2016.
15. Balanis, C. A., *Antenna Theory: Analysis and Design*, John Wiley Sons, Hoboken, NJ, 2012
16. Hussain, R., M. S. Sharawi, and A. Shamim, "An integrated four-element slot-based MIMO and a UWB sensing antenna system for CR platforms," *IEEE Trans. Antennas Propag.*, Vol. 66, No. 2, 978–983, 2018.
17. Devi, G. A., J. Aarthi, P. Bhargav, R. Pandeewari, M. A. Reddy, and R. S. Daniel, "UWB frequency reconfigurable patch antenna for cognitive radio applications," *2017 IEEE International Conference on Antenna Innovations Modern Technologies for Ground, Aircraft and Satellite Applications (iAIM)*, 2017.
18. Pahadsingh, S., S. Sahu, and S. Das, "Compact ultrawideband-reconfigurable antenna for cognitive radio platforms," *2017 International Conference on Wireless Communications, Signal Processing and Networking (WiSPNET)*, 2735–2738, 2017.
19. Golliwar, A. V. and M. S. Narlawar, "Multiple controllable band notch butterfly shaped monopole UWB antenna for cognitive radio," *2016 World Conference on Futuristic Trends in Research and Innovation for Social Welfare (Startup Conclave)*, 2016.

20. Sahnoun, N., I. Messaoudene, T. A. Denidni, and A. Benghalia, "Integrated flexible UWB/Nb antenna conformed on a cylindrical surface," *Progress In Electromagnetics Research Letters*, Vol. 55, 121–128, 2015.
21. Kumar, N. A. and A. S. Gandhi, "A compact novel three-port integrated wide and narrowband antennas system for cognitive radio applications," *International Journal of Antennas and Propagation*, 1–14, 2016.
22. Zheng, S., X. Liu, and M. M. Tentzeris, "A novel optically controlled reconfigurable antenna for cognitive radio systems," *2014 IEEE Antennas and Propagation Society International Symposium (APSURSI)*, 2014.
23. Erfani, E., J. Nourinia, C. Ghobadi, M. Niroo-Jazi, and T. A. Denidni, "Design and implementation of an integrated UWB/reconfigurable-slot antenna for cognitive radio applications," *IEEE Antennas Wireless Propag. Lett.*, Vol. 11, 77–80, 2012.
24. Ebrahimi, E., J. R. Kelly, and P. S. Hall, "Integrated wide-narrowband antenna for multistandard radio," *IEEE Trans. Antennas Propag.*, Vol. 59, No. 7, 2628–2635, 2011.
25. Tawk, Y. and C. Christodoulou, "A new reconfigurable antenna design for cognitive radio," *IEEE Antennas Wireless Propag. Lett.*, Vol. 8, 1378–1381, 2009.